# Injection of anomalous-Hall current into a load circuit

D. Lacour, M. Hehn, Min Xu, J.-E. Wegrowe

▶ **To cite this version:**

D. Lacour, M. Hehn, Min Xu, J.-E. Wegrowe. Injection of anomalous-Hall current into a load circuit. Journal of Applied Physics, 2024, 135 (19), pp.193903. 10.1063/5.0205911 . hal-04585745

**HAL Id: hal-04585745**
**https://hal.science/hal-04585745**

Submitted on 23 May 2024

**HAL** is a multi-disciplinary open access archive for the deposit and dissemination of scientific research documents, whether they are published or not. The documents may come from teaching and research institutions in France or abroad, or from public or private research centers.

L'archive ouverte pluridisciplinaire **HAL**, est destinée au dépôt et à la diffusion de documents scientifiques de niveau recherche, publiés ou non, émanant des établissements d'enseignement et de recherche français ou étrangers, des laboratoires publics ou privés.

Distributed under a Creative Commons Attribution 4.0 International License

ACCEPTED MANUSCRIPT

Journal of Applied Physics

This is the author's peer reviewed, accepted manuscript. However, the online version of record will be different from this version once it has been copyedited and typeset.
PLEASE CITE THIS ARTICLE AS DOI: 10.1063/5.0205911

AIP Publishing

# Injection of anomalous-Hall current into a load circuit

D. Lacour,[1] M. Hehn,[1] Min Xu,[1] and J.-E. Wegrowe[2, a)]
[1)] *Institut Jean Lamour UMR 7198 CNRS, Université de Lorraine, Vandoeuvre les Nancy France*
[2)] *Laboratoire des Solides Irradiés, Ecole polytechnique, CNRS, CEA, Université Paris-Saclay, F 91128 PALAISEAU, France*

(Dated: 10 April 2024)

The anomalous-Hall current injection is studied in a Hall device contacted to a lateral load circuit. This anomalous-Hall current is generated inside a $Co_{75}Gd_{25}$ ferrimagnetic Hall bar and injected into a lateral load circuit contacted at the edges. The current, the voltage and the power are measured as a function of the magnetization states, the load resistance $R_l$, and the temperature. It is shown that (1) the resistance associated with the anomalous-Hall current flowing inside the Hall bar is that of the portion of the ferrimagnet located between the lateral contacts, (2) the role of the non-uniformity of the current due to the lateral contacts is small, (3) the maximum power efficiency of the current injection into the load circuit corresponds to the condition of the resistance matching of the two sub-circuits, and (4) this maximum power efficiency is of the order of the square of the anomalous-Hall angle. These observations are in agreement with recent predictions based on a non-equilibrium variational approach.

PACS numbers: 72.25.Mk, 85.75.-d

## I. INTRODUCTION

The search for low power consumption electronic devices is one of the main motivation for the development of spintronics. Indeed, the spins attached to the charge carriers allow a direct manipulation of the magnetization states. Accordingly, the power used is that of the spin degrees-of-freedom, and not directly the electric power. Yet the transport of the spins attached to the charge carriers follows the thermodynamic rules that determines Joule dissipation. In the case of Hall effect (HE), anomalous Hall effect (AHE)[1–7], or spin-Hall effect (SHE)[8], the Joule dissipation is minimized due to the presence of an effective magnetic field that breaks the time-invariance symmetry at the microscopic scale[9]. The effect of the effective magnetic field on the electric carriers is then taken into account by a typical supplementary Hall-like term in the Ohm's law[10–12] (see Eq.(1) below).

It is well-known that the force associated with a magnetic field - typically the Lorentz force for the HE - cannot produce mechanical work in vacuum. More generally, due to the Onsager reciprocity relations, it is often assumed that the Hall-current produced by Hall-like effects is dissipationless[13–18]. However, it is not necessarily the case: typically, the power associated with the Hall voltage in a perfect Hall bar is indeed null, but the power associated with a Corbino disk (all other things being equivalent) dissipates[12,19]. The Hall bar contacted to a lateral circuit presents an intermediate state between these two limiting cases of zero load resistance (Corbino disk) and infinite load resistance (perfect Hall bar).

The injection of spin-current produced by SHE or AHE has attracted much attention in the context of spin-orbit torque (SOT) effects, or charge-to-spin conversion mechanisms. Indeed, SOT allows a ferromagnetic layer to be reversed by the injection of spin-polarized current from an adjacent non-magnetic Hall bar (for the SHE) or from an adjacent magnetic Hall bar (for the AHE)[20–24]. The SOT device is hence related to the Hall bar contacted to a lateral load circuit as described above (the lateral layer would then play the role of the lateral resistance). However, in the literature, the parameter used so far for the evaluation of the power efficiency is the Joule dissipation $J_{sw}^2\rho$ that is generated by the switching current density $J_{sw}$ injected from the generator (or $\rho/\theta_{sot}^2$ as shown in the Fig.8 of the review *Roadmap of SpinOrbit Torques*[25]), without taking into account the load resistance of the adjacent ferromagnetic layer.

The goal of the present report is to study the anomalous Hall-current that flows inside the Hall bar, and the conditions that govern the injection of this current into a load circuit. In the experimental protocol proposed here (see Fig.1), the load circuit is devoted to measure the amount of Joule power injected from the ferrimagnetic layer due to the AHE, regardless of the spin properties[26].
It is shown that the transverse resistance experienced by the anomalous-Hall current flowing from one edge to the other edge inside the sample is defined by the resistivity $\rho$ of the ferrimagnet and the section defined by the lateral electrodes. The role of the non-homogeneity of the current lines due to the electrodes is not significant (it is characterized by the pink zone in Fig.3b below). Furthermore, the power efficiency is measured to be of the order of the square of the anomalous Hall angle $\theta_{AH}^2 \sim 10^{-5}$ and a sharp maximum is observed, that corresponds to the resistance matching between the magnetic layer and

[a)] Electronic mail: jean-eric.wegrowe@polytechnique.edu

ACCEPTED MANUSCRIPT
Journal of Applied Physics
AIP Publishing
This is the author's peer reviewed, accepted manuscript. However, the online version of record will be different from this version once it has been copyedited and typeset.
PLEASE CITE THIS ARTICLE AS DOI: 10.1063/5.0205911

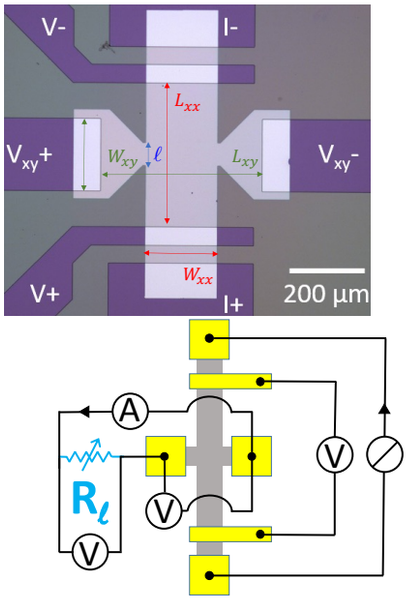


FIG. 1. : (a) Picture of the *CoGd* Hall bar, with the Au contact pads. An electric generator (not shown) imposes a constant current through the vertical bar ($x$ direction). A transverse anomalous-Hall current is generated inside the ferrimagnet, and injected through the lateral electrodes ($y$ direction). (b) Complete circuit with ferrimagnetic Hall-bar (grey) and the lateral load resistance $R_l$, the longitudinal-current generator and the position of the ammeter and the voltmeters.

the load circuit. Note that these observations are not trivial because the system does not obey the Kirchhoff's laws and cannot be described by a simple lumped-resistor circuit[27]. These observations are in agreement with recent predictions based on a non-equilibrium variational approach[28–30]. Beside, these results show that - like for direct spin-injection into semiconductors[31,32] - the impedance matching could also be a crucial issue for transverse spin-current injection into the adjacent layers of a Hall-bar for SOT.

## II. EXPERIMENTAL PROTOCOL AND RESULTS

The samples is a $Co_{75}Gd_{25}$ layer of thickness $t = 30$ nm, sputtered on a glass substrate and the buffer layer. The choice of the ferrimagnet $Co_{75}Gd_{25}$ is motivated by its high amplitude of $AHE$, its negligible planar Hall effect (i.e. its negligible anisotropic magnetoresistance) and its negligible magnetocrystalline anisotropy[12]. The magnetic layer is sandwiched between 5 nm thick Ta buffer and 3 nm thick Pt cap. As shown in Fig.1, the length of the Hall bar is $L_{xx} = 400\,\mu m$ and the width $W_{xx} = 200\,\mu m$. The magnetic properties and the transport properties of the thin layers have been previously studied (see Supplementary Materials[10]). The magnetization is uniform for the quasi-static states, which are the only states under consideration in this study. The out-of-plane shape anisotropy corresponds to a field of about $0.8\ T$ defined by the magnetization at saturation. The structure of CoGd is amorphous and there is no texture. The study of the magnetization states are presented in the Supplementary Materials[10].

At room temperature the longitudinal voltage is $\Delta V = 0.148\ V$, the longitudinal current flowing through the CoGd is $0.43\ mA$ and the resistance of the layer is $R_{CoGd} \approx 344\ \Omega$. The anomalous Hall voltage per Tesla is $V^0_{xy} = 0.886\ mV\ T^{-1}$ (the index $^0$ sands for the open lateral circuit). The anomalous Hall angle per Tesla $\theta_{AH} = \frac{V^0_{xy}}{\Delta V} = 6\ 10^{-3}\ T^{-1}$ is deduced, leading the value of the anomalous resistivity per Tesla of about $\rho_{AH} \approx 1.02\,10^{-2}\ \mu\Omega.m.T^{-1}$.

Gold contact pads are formed thanks to a standard 2 steps UV lithographic process (yellow pads shown in Fig.1b). As shown in Fig.(1), the pads at the extremity along the $x$ axis of the Hall bar allow the $Co_{75}Gd_{25}$ layer to be contacted to the electric generator, and two opposite lateral pads at the edges ($L_{xy} = 450\ \mu$m and $W_{xy} = 200\ \mu m$) define the lateral terminals for the load resistances $R_l$, range between $1\Omega$ and $100k\Omega$ (decade resistance box). Voltmeters and ampermeter allow the lateral voltage $V_{xy}$ and the lateral current $I_{xy}$ to be measured while injecting a DC longitudinal current (see Figure 1). An external magnetic field $H_{app}$ varying between $\pm 1.5\ T$ is applied at an angle $\Phi_{\rm Happ}$ defined with respect to the direction of the injected current $I_{xx}$.

Figure 2 shows the lateral voltage $V_{xy}$ (Fig.2a), the lateral current $I_{xy}$ (Fig.2b) and the power $P = V_{xy}I_{xy}$ (Fig.2c) measured on the load circuit and plotted as a function of the amplitude of the magnetic field at $\Phi_{\rm Happ} = 90^o$ (applied normal to the layer) at room temperature. The load resistance $R_l$ is used as a parameter, depicted in the color code shown in the right (green for $1\ \Omega$ up to red for $8000\ \Omega$).

Figure 2d shows the profiles of the anomalous Hall current as a function of the angle $\Phi_{\rm Happ}$ in a load resistance of $R_l = 270\,\Omega$ (close to the maximum of the power in the profile of Figure 3b), for three different amplitudes of the applied field. At $H_{app} = 1.5\ T$ (at saturation), the magnetization direction $\vec{m}$ follows approximately the applied field. For $H_{app} < 1$ Tesla, the angle of the magnetization and that of the magnetic field are significantly different due to the shape anisotropy[10].

The continuous lines in Fig.2d corresponds to the angular profile of the AHE: $V_{xy}(\vec{H}_{app}) \propto \vec{m}(\vec{H}_{app}).\vec{e}_z$ where $\vec{m}$ is the magnetization direction and $\vec{e}_z$ gives the direction normal to the plane of the Hall bar. The contribution of the Planar Hall effect (PHE) of the *CoGd* layer is about two orders of magnitude below the AHE and can be neglected[10]. The important point is that the observed profiles show a typical signature of the AHE. It is worth pointing-out that the analysis about AHE in Fig.2d is performed on the measurement of the anomalous-Hall *current* injected in the lateral circuit, and not on the *voltage* of the open circuit: such studies have not been

ACCEPTED MANUSCRIPT
Journal of Applied Physics
AIP Publishing
This is the author's peer reviewed, accepted manuscript. However, the online version of record will be different from this version once it has been copyedited and typeset.
PLEASE CITE THIS ARTICLE AS DOI: 10.1063/5.0205911



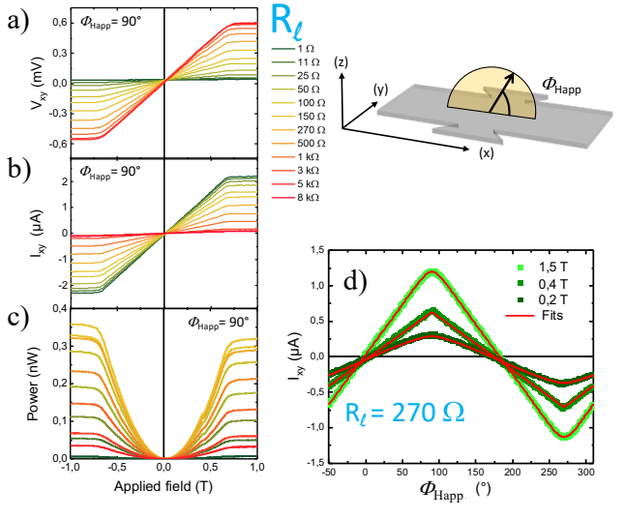


FIG. 2. : (a) Voltage $V_{xy}$ and (b) current $I_{xy}$ measured at the terminals of the load resistance $R_l$ as a function of the magnetic field applied perpendicular to the ferrimagnetic layer. (c) The Joule Power $P = I_{xy}V_{xy}$ measured as a function of the load resistance $R_l$. (d) Current $I_{xy}$ measured as a function of the angle $\Phi_{\rm Happ}$ of the applied field at load resistance $R_l = 270\,\Omega$ for three values of the amplitude of the applied field. The continuous lines are calculated from the AHE.

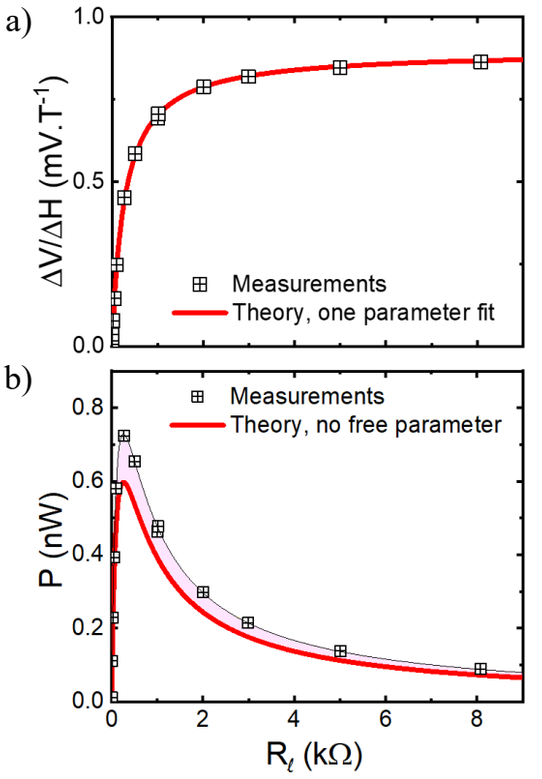


FIG. 3. : (a) Voltage $V_{xy}$ per unit of magnetic field plotted as a function of the load resistance $R_l$. The line is a one parameter fit from Eq.(2), with the geometric adjustable parameter $\alpha$. (b) Measured electric power $P$ as a function of the load resistance (squares). The lines are the calculation deduced from Eq.(3). The quantitative shift in pink is attributed to the curvature of the current lines due to the lateral contacts.

reported in the literature so far (to the best of our knowledge).

The calculation of $\vec{m}(\vec{H}_{app})$ and the details of the magnetic simulation are presented in the supplementary materials[10] and in references[12]. The excellent agreement between the fit and the data in Fig.2d - together with the specificity of AHE profiles - confirm that the current measured in the load circuit is due uniquely to the anisotropic Hall current generated by the AHE of the ferrimagnetic layer.

As can be seen in Fig.2a, when a load resistance $R_l$ is contacted to the edges, the amplitude of the anomalous Hall voltage $V_{xy}$ is a monotonous increasing function of $R_l$. In contrary, the anomalous hall current injected into the lateral circuit is a monotonous decreasing function of $R_l$. This is compatible with the intuitive interpretation that the electric charges accumulated at the edges of the Hall bar - that is a consequence of the AHE - are extracted and injected into the load circuit in proportion of the load resistance.

Note that the sign of the anomalous-Hall current is inverted when the direction of the magnetization is changed. This is a consequence of the change of the sign of the accumulated charges when the magnetization is rotated from up to down direction (this sign is equally inverted when the direction of the longitudinal current is reversed). The profile of power shown in Fig.2d is well-characterized by a quadratic shape interrupted by the two horizontal lines corresponding to the up and down saturation states of the magnetization[33]. In Fig.3a the voltage variation (in Volt per Tesla) is plotted as a function of the load resistance $R_l$. On the other hand, Fig.3b shows the profile of the Joule power dissipated in the load resistance. The profile of the power is no longer a monotonous function of the load resistance and a sharp maximum appears for a well-defined resistance. The two typical profiles shown in Fig.3a and Fig.3b are analyzed in the next section.

## III. ANALYSIS

The transverse Hall-current is zero for the open circuit. In contrast, if the Hall bar is in contact to the load circuit, an anomalous-Hall current is generated, that injects the charge carriers accumulated at the edges into

ACCEPTED MANUSCRIPT
Journal of Applied Physics
AIP Publishing
This is the author's peer reviewed, accepted manuscript. However, the online version of record will be different from this version once it has been copyedited and typeset.
PLEASE CITE THIS ARTICLE AS DOI: 10.1063/5.0205911

the load circuit. The anomalous-Hall voltage decreases accordingly, as seen in Fig.2a. At stationary regime, the out-of-equilibrium balance between the charge accumulation and current injection into to the load circuit is determined by the principle of minimum power dissipation under the contraints imposed to the system[34]. This scenario is investigated in the reference[29] *Faisant et al, JAP 2021* for the usual Hall effect in a perfect Hall bar (assuming the invariance by translation along the longitudinal direction $x$). The main results are summarized below.

The generalized Ohm's law relates the electric current density $\vec{J} = \{J_x, J_y, J_z\}$ to the electrochemical potential $\mu$. The gradient $\vec{\nabla}\mu$ of the electrochemical potential is used instead of the electric field in order to include the effect of the electric screening[29]. The Hall-device is defined in the plane $\{x, y\}$, in which $x$ is the longitudinal direction defined by the current injection from the generator, $y$ is the transverse direction, and $z$ is the direction perpendicular to the plane of the layer. The Ohm's law then reads:

$$\vec{J} = -\sigma \left( \vec{\nabla}\mu - \theta_{AH}\, \vec{e_z} \times \vec{\nabla}\mu \right), \tag{1}$$

where $\times$ denotes the cross product, $\vec{\nabla} = \{\partial_x, \partial_y, \partial_z\}$ is the gradient, $\sigma = 1/\left(\rho\left(1+\theta_{AH}^2\right)\right)$ is the conductivity of the *CoGd* ferrimagnetic layer[10] while $\theta_{AH}$ is the anomalous Hall angle introduced above. The total electric power dissipated in the device is given by $P = \int \vec{J}.\vec{\nabla}\mu\, dv$ (integrated over the volume of the device). After performing the functional minimization of the electric power $P$ under the two constraints of global charge conservation and global current conservation, the Hall voltage at the edges is given by the expression (for constant temperature and small charge accumulation)[29]:

$$V_{xy}(R_l) = V_{xy}^0 \frac{1}{1+\frac{\rho}{\alpha R_l}}, \tag{2}$$

where $\rho$ is the resistivity of the CoGd layer and the unknown *geometrical parameter* $\alpha$ is such that the ratio $\rho/\alpha$ defines the resistance $R$ of the active region of the ferrimagnetic Hall cross. The fit of the data in Fig.3a with the adjustable parameter $\alpha = 0.93\,10^{-8}\ m$ is given by the red curve. This coefficient $\alpha \approx (\ell\, t)/W_{xx}$ defines the geometry of the lateral current injection through the *active part* of the sample, as shown in Fig.1a. Indeed, the anomalous-Hall current is injected through the effective section $\ell.t$ where $t = 3\ 10^{-8}$ m is the thickness of the sample, $\ell$ is the size of the lateral pad in contact to the Hall bar, and $W_{xx} = 3\ell$. It is worth pointing-out that the transverse resistance $R$ experienced by the anomalous Hall current while flowing from one edge to the other inside the sample is defined by the resistivity $\rho$ of the ferrimagnet and the section located between lateral electrodes. As pointed-out in the introduction, this is not a trivial result because the Hall-device cannot be described by a simple lumped-resistor circuit[18,27].

On the other hand, the expression of the power dissipated in the load circuit reads[29]:

$$P(R_l) = P_0\, \theta_{AH}^2 \frac{\frac{\rho}{\alpha R_l}}{\left(1+\frac{\rho}{\alpha R_l}\right)^2} \tag{3}$$

where $P_0 \approx 64\,\mu W$ is the input power injected from the electric generator into the CoGd Hall bar. This value takes into account the correction due to the current flowing through the buffer layer and through the cap layer. The profile of the power $P(R_l)$ (Eq.(3)) is calculated and plotted in Fig.3b (continuous line), together with the measured power (squares).

As can be seen in Fig.3, the measurements are qualitatively in agreement with the model. A sharp maximum is measured for a load resistance equal to the resistance $R_l = R = \rho/\alpha$. The pink zone between the calculated curve and the experimental points shows a global shift between the measurements and the theory. It is surprising to see that the calculated profile is below the measured profile, since the model is based on an optimized ideal Hall-bar (invariant by translation), for which the maximum efficiency is expected. We ascribe the shift to the under-estimation of the measured anomalous Hall angle $\theta_{AH}$, which is due to the inhomogeneity of the current lines near the lateral contacts. This counter-intuitive effect has been discussed in the context of spin-Hall measurements[35], and is studied in the supplementary materials[10]. After performing this correction, the calculated curve can be superimposed to the experimental points.

This observation hence validates qualitatively and quantitatively the prediction derived in reference[29], and confirms the general assumption that the anomalous-Hall current (like the Hall current) is very sober in terms of power consumption (of the order of $\theta_{AH}^2$ times the power injected in the Hall bar), but invalidate the claim that it is dissipationless for a perfect Hall bar.

Before concluding it is important to point-out that - as shown in Fig.4 - the same measurements performed at different temperatures, from $T = 30\ K$ to $T = 295\ K$, does not change the profiles (described by Eqs.(2) and Eq.(3)). There is no qualitative change in the dissipation regime for the temperature range under consideration. In our context, the temperature dependence of the power is defined by the temperature dependence of the parameters $\theta_{AH}$ and $\rho$ in Eq.(3), whatever the mechanism responsible for the presence of the effective magnetic field : either spin-orbit coupling or Berry curvature (as discussed in references[1–6]).

## IV. CONCLUSION

In conclusion, the anomalous-Hall current flowing inside a ferrimagnetic GdCo layer and the electric power generated by this current into a load circuit have been studied

ACCEPTED MANUSCRIPT
Journal of Applied Physics
AIP Publishing
This is the author's peer reviewed, accepted manuscript. However, the online version of record will be different from this version once it has been copyedited and typeset.
PLEASE CITE THIS ARTICLE AS DOI: 10.1063/5.0205911



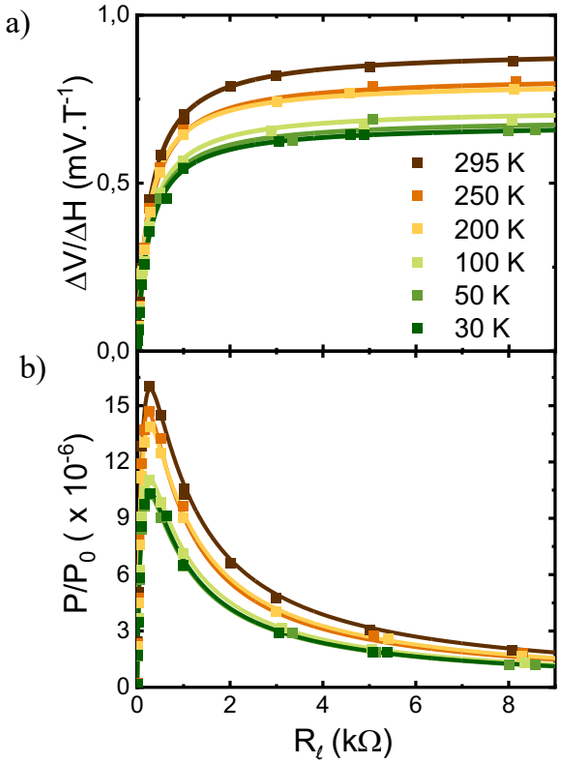


FIG. 4. : (a) Voltage $V_{xy}$ per unit of magnetic field and (b) Normalized electric power $P/P_0$ as a function of the load resistance $R_l$ for six different temperatures.

as a function of the magnetization states $\Phi_{\text{Happ}}$, the load resistance $R_l$ and the temperature $T$. The experimental protocol allows the physical properties of the transverse anomalous Hall current to be characterized and quantified.

The observations show that the Hall-current behaves as a usual current inside the ferrimagnetic layer (resistance $R = \rho\alpha$), and the maximum electric-power dissipated in the load circuit is indeed very small, of the order of the square of the anomalous-Hall angle $\theta_{AH}^2$. Furthermore, the profile shows a sharp maximum corresponding to the resistance matching. The matching occurs when the resistance of the load circuit $R_l$ equals the resistance $R$ of the *active part* for AHE, defined by the geometrical parameter $\alpha \approx \ell t/W_{xx}$. This result is not trivial, because the system cannot be described by the Kirchhoff's laws (i.e. by a lumped-resistor circuit)[18,27].

Finally, it is important to point-out that the presence of a sharp peak in the profile of the power injected in the load circuit could have important consequences for the optimization of SOT. Indeed, the power carried by the spins in a spin-current is supposed to be controlled by the Joule power carried by the electric charges. The resistance $R_l$ is suspected to play a crucial role in the efficiency of the spin-injection, which could be drastically reduced in case of impedance mismatch. This study suggests that for the optimization of SOT devices, the ensemble of writing processes could be separated into an upstream anomalous-Hall transducer that transforms a part of the electric power of the generator into the Hall current (Eq.(3)), and a downstream charge-to-spin converter that uses the spin-polarization of the current in order to switch a magnetic layer located at nanoscopic distance from the Hall bar.

## V. SUPPLEMENTARY MATERIAL

The supplementary Material[10] contains four sections, that complement the main text. The corresponding information is not necessary for the understanding of the message delivered in the present report, but it presents the magnetic and electric properties of the samples (Section I, II and III), and discusses some basic questions related to the context of the study (Section IV).

- Section I ( *"Magnetic characterization and simulation"*) presents and discusses the magnetic characterization of the GdCo layer, together with the corresponding magneto-transport properties: anisotropic magnetoresistance (AME), planar Hall effect (PHE), and anomalous Hall effect (AHE). The characterization allows the values of the parameters used in the main text to be defined.
- Section II ( *"Resistance and resistivity"*) establishes the resistance of the $CoGd$ layer from the total longitudinal resistance, that includes the $Pt$ cap layer and the $Ta$ buffer layer.
- Section III ( *"Correction of $\theta_{AH}$ due to the real geometry"*) discusses the deviation of the current lines from the uniform longitudinal current density $J_x^0$ due to the presence of the lateral contacts. This estimation explains the deviation (pink zone) observed on the Fig.3a.
- Section IV (*"Overlooked properties about dissipation in Hall and Anomalous Hall devices"*) presents some important and basic questions about dissipation in Hall devices, in the spirit of the present study. In principle, these general results should be known at the basic level, but they are surprisingly overlooked in the textbooks about solid-state physics, semiconductor physics, or monographs about Hall devices.

[1] R. Karplus and J. M. Luttinger, *Hall Effect in Ferromagnetics*, Phys. Rev. **95** 1154 (1954).
[2] J. Kondo, *Anomalous Hall Effect and Magnetoresistance of Ferromagnetic Metals*, Prog. Theo. Phys. **27** 772 (1962).
[3] L. Berger, *Side-Jump Mechanism for the Hall Effect in Ferromagnets*, Phys. Rev. B **2** 4559 (1970).
[4] Ph. Nozières and C. Lewiner, *A simple theory of the anomalous Hall effect in semiconductors*, J. de Physique **34** (1973) 901.
[5] A. Crepieux and P. Bruno *Theory of anomalous Hall effect from the Kubo formula and the Dirac equation*, Phys. Rev. B **64**, (2001) 014416.

ACCEPTED MANUSCRIPT
Journal of Applied Physics
AIP Publishing
This is the author's peer reviewed, accepted manuscript. However, the online version of record will be different from this version once it has been copyedited and typeset.
PLEASE CITE THIS ARTICLE AS DOI: 10.1063/5.0205911

[6]F. D. M. Haldane *Berry Curvature on the Fermi Surface: Anomalous Hall Effect as a Topological Fermi-Liquid Property*, Phys. Rev. Lett. **93**, 206602 (2004)

[7]N. Nagasoa et al. *Anomalous Hall effect*, Rev. Mod. Phys. **82**, 1539 (2010).

[8]J. Sinova et al. *Spin Hall effects* Rev. Mod. Phys. **87**, 12131260 (2015).

[9]L. Onsager *Reciprocal Relations in Irreversible Processes II*, Phys. Rev. **38** 2265 (1931).

[10]Supplementary materials.

[11]J.-E. Wegrowe, D. Lacour, H.-J. Drouhin *Anisotropic magnetothermal transport and spin Seebeck effect*, Phys. Rev. B **89**, 094409 (2014).

[12]B. Madon et al. *Corbino magnetoresistance in ferromagnetic layers : Two representative examples* $Ni_{81}Fe_{19}$ *and* $Co_{83}Gd_{17}$, Phys. Rev B (R) **98**, 220405(R) (2018).

[13]Wei-Li Lee et al. *Dissipationless Anomalous Hall Current in the Ferromagnetic Spinel* $CuCr_2Se4 - xBr_x$, Science **303** 1648 (2004).

[14]Jairo Sinova et al. *Universal Intrinsic Spin Hall Effect* , Phys. Rev. Lett. **92**, 126603 (2004).

[15]Y. Onose, Y. Shiomi, and Y. Tokura *Dissipationless Nature of the Anomalous Hall Effect in Itinerant Ferromagnets*, Phys. Rev. Lett. **100**, 016601 (2008).

[16]M. Meng, S. X. Wu, W. Q. Zhou, L. Z. Ren, Y.J. Wang, G. L. Wang, and S. W. Li, *Anomalous Hall effect in epitaxial ferrimagnetic anti-perovskite* $Mn_{4-x}Dy_xN$ *films* J. Appl. Phys. **118**, 053911 (2015).

[17]Di Yue, Xiaofeng Jin *Towards a Better Understanding of the Anomalous Hall Effect*, J. Phys. Soc. Jpn. **86**, 011006 (2017).

[18]Giovanni Viola and David P. DiVincenzo, *Hall Effect Gyrators and Circulators*, Phys. Rev. X **4**, 021019 (2014).

[19]R. Benda, J.-E. Wegrowe, M. J. Rubì, *Towards Joule heating optimization in Hall devices*, Phys. Rev. B **98**, 085417 (2018).

[20]Tomohiro Taniguchi, Julie Grollier, M. D. Stiles, *Spin-Transfer Torques Generated by the Anomalous Hall Effect and Anisotropic Magnetoresistance*, Phys. Rev. Appl. **3**, 044001 (2015).

[21]Rahul Mishra et al. *Anomalous Current-Induced Spin Torques in Ferrimagnets near Compensation* Phys. Rev. Lett. **118**, 167201 (2017).

[22]Hao Wu et al. *Spin-orbit torque from a ferromagnetic metal*, Phys. Rev. B **99**, 184403 (2019).

[23]A. Manchon et al. *Current-induced spin-orbit torques in ferromagnetic and antiferromagnetic systems*, Rev. Mod. Phys. **91**, 035004 (2019).

[24]Jeongchun Ryu et al. *Current-Induced Spin-Orbit Torques for Spintronic Applications*, Advanced Materials, **32**, Issue 35 (2021).

[25]Qiming Shao et al., *Roadmap of SpinOrbit Torques*, EEE Trans. Mag. **57** (7) 800439 (2021)

[26]The measurement of the spin-dependent properties of the anomalous-Hall current in the present experiments would have necessitate to scale down the load circuit at the nanoscopic scale, as performed in the case of the SHE in the reference: Y. Omori; F. Auvray; T. Wakamura; Y. Niimi; A. Fert; Y. Otani, Appl. Phys. Lett. **104**, 242415 (2014).

[27]The best proof about this assertion is that the results presented here are not equivalent to that obtained in the case of the Planar Hall Effect (PHE) with identical Hall angle and identical device geometry. Indeed, the Kirchhoff's laws impose the same lumped-element circuit for both PHE and AHE, while the two transport equations are significantly different (the conductivity matrix for PHE is symmetric instead of antisymmetric for AHE). The comparative study between AHE and PHE is treated in a forthcoming article (ArXiv 2024).

[28]M. Creff, F. Faisant, M. Rubì, J.-E. Wegrowe *Surface current in Hall devices*, J. Appl. Phys. **128**, 054501 (2020). https://doi.org/10.1063/5.0013182.

[29]F. Faisant, M. Creff, J.-E. Wegrowe *The physical properties of the Hall current*, J. Appl. Phys. **129**, 144501 (2021), https://doi.org/10.1063/5.0044912

[30]M. Creff, E. Olive, and J.-E. Wegrowe, *Screening effect in Spin-Hall Devices*, Phys. Rev. B **105**, 174419 (2022).

[31]G. Schmidt, D. Ferrand, A. T. Filip and B. J. van Wees and L. W. Molenkamp *Fundamental obstacle for electrical spin injection from a ferromagnetic metal into a diffusive semiconductor* Phys. Rev. B **62** R4790 (2000).

[32]A. Fert and H. Jaffrès, *Conditions for efficient spin injection from a ferromagnetic metal into a seminconductor* Phys. Rev. B **64**, 184420 (2001).

[33]The small asymmetry between $\pm 1.5\ T$ fields is due to small offset voltage and current generated at the outside contacts.

[34]L. Onsager and S. Machlup, *Fluctuations and irreversible processes*, Phy. Rev. **91**, 1505 (1953).

[35]Lukas Neumann and Markus Meinert, *Influence of the Hall-bar geometry on the harmonic Hall voltage measurements of spin-orbit torques*, AIP Advances **8**, 095320 (2018).